

PAPER

Experimental Evaluation of Passive MIMO Transmission with Load Modulation for RFID Application

Keisuke TERASAKI^{†a)}, Student Member and Naoki HONMA[†], Member

SUMMARY This paper describes experiments on passive Multiple-Input Multiple-Output (MIMO) transmission with load modulation. PIN diodes are used as the variable impedance element at the tag side to realize multi-level modulation. The results indicate that the transmission rate of passive MIMO is up to 2 times higher than that of Single-Input Single-Output (SISO) with the same transmission power when the distance between the reader and the tag is 0.5 m. Also, when the distance is 1 m, MIMO offers up to 1.7 times higher transmission rate than SISO. These results indicate that passive MIMO offers high-speed data transmission even when the distance is doubled.

key words: MIMO, RFID, load modulation, multilevel modulation

1. Introduction

Radio Frequency Identification (RFID) has attracted much attention as the alternative to bar code readers. RFID is a very practical technology for identifying and managing people and goods using small wireless chips called tags; current applications include travel cards, employee ID cards, and electronic money. Passive RFID systems, the dominant type, use load modulation [1] to establish a channel from tag to reader. Load modulation enables the tag to transmit its information to the reader by controlling the reflection of waves by altering the tag side's load impedance. Passive RFID has the advantage that it eliminates the transmitter from the tag side, but conventional load modulation schemes employ single antennas and on-off-keying, and so cannot attain high-speed data transmission. Thus recent demands for low power and high-speed data rates remain unsatisfied.

One solution is to set multiple antennas in the reader and the tag, see Fig. 1(b) [2], [3]; Fig. 1(a) shows the conventional single antenna. By using multiple antennas, multiple signals can be transmitted in parallel [4]–[6]. It offers high-speed data transmission not by extending the bandwidth but by spatial-multiplexing [7], [8]. But studies [2] and [3] use only binary on/off keying.

For further increase of the transmission data rates, we have proposed the passive MIMO technique, a high-speed data transmission method that uses load modulation and multiple antennas in both reader and tag, and multilevel modulation that improves the bits carried per symbol. We set the load impedance in stages to establish many reflection coefficients rather than binary on/off [9]–[11]. We proved

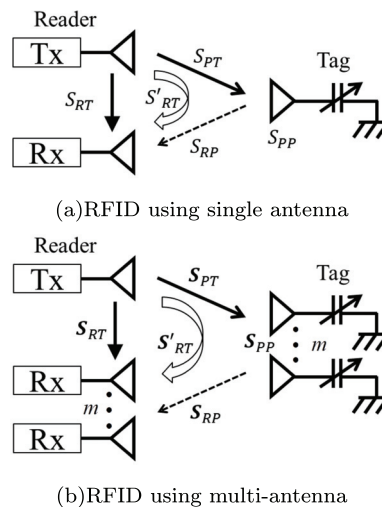


Fig. 1 RFID system.

the validity of this method mainly by simulation, but no experiments were conducted at that time.

2. Experimental Setup

2.1 Passive MIMO Transmission with Load Modulation

In passive RFID, the reader transmits an unmodulated continuous wave. This wave is reflected at the tag side, and then captured by the reader. At the tag side antenna, the load impedance is altered to control the amplitude and phase of the reflected wave. The reader can detect the presence and state of the tag from the reflected wave, and acquire the data held by the tag.

In passive MIMO, multiple signals can be reflected in parallel by the multiple antennas. Figure 1(b) shows the system model of passive MIMO. In this figure, m refers to the reader-receiver and tag antennas. The configurations with $m = 1$ and $m = 2$ mean SISO and MIMO, respectively. The number of reader-transmitter antennas is 1 in this study.

In this paper, T, P, and R represent the transmitting, tag, and receiving ports, respectively. Figure 2 shows the scattering matrix model explaining this antenna system. Here, a_T is the transmitted signal from T port, $a_P = [a_{P1}, \dots, a_{Pm}]^T$ is the signals from P port, $b_R = [b_{R1}, \dots, b_{Rm}]^T$ is the signals to R port, and $b_P = [b_{P1}, \dots, b_{Pm}]^T$ is the signals to P port, where $[\cdot]^T$ is the matrix transposition. The relationship between b_R and b_P can be expressed as

Manuscript received November 29, 2013.

Manuscript revised March 16, 2014.

[†]The authors are with the Graduate School of Engineering, Iwate University, Morioka-shi, 020-8551 Japan.

a) E-mail: t2312026@iwate-u.ac.jp

DOI: 10.1587/transcom.E97.B.1467

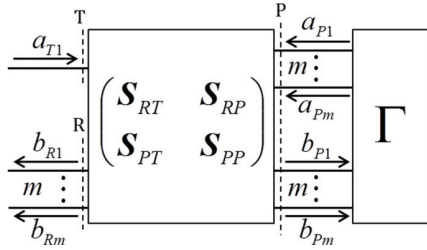


Fig. 2 Scattering matrices equivalent model.

$$\Gamma \mathbf{b}_P = \mathbf{a}_P \quad (1)$$

$$\begin{pmatrix} \mathbf{b}_R \\ \mathbf{b}_P \end{pmatrix} = \begin{pmatrix} S_{RT} & S_{RP} \\ S_{PT} & S_{PP} \end{pmatrix} \begin{pmatrix} \mathbf{a}_T \\ \mathbf{a}_P \end{pmatrix} \quad (2)$$

where S_{RT} , S_{RP} and S_{PT} are the scattering matrices that denote the channels among T, P, and R ports. S_{PP} are the scattering matrices that denote the reflection and coupling coefficients at the tag antenna. From the relationship shown in (1) and (2), the observed signal at port R is described as,

$$\begin{aligned} \mathbf{b}_R &= \left\{ S_{RT} - S_{RP} (S_{PP} - \Gamma^{-1})^{-1} S_{PT} \right\} \mathbf{a}_T \\ &= S'_{RT} \mathbf{a}_T \end{aligned} \quad (3)$$

where S'_{RT} ($m \times 1$) is the channel between T and R. The reflection coefficient of the termination loads is given as

$$\Gamma = \text{diag} \left(\frac{Z_1 - Z_0}{Z_1 + Z_0}, \dots, \frac{Z_m - Z_0}{Z_m + Z_0} \right) \quad (4)$$

where Z_1, \dots, Z_m correspond to the load impedance values of tag antennas 1, \dots, m , respectively, and Z_0 is the reference impedance. In this paper, PIN diodes are used as the variable impedance elements at the tag side; their impedance is set by changing the applied current i.e., Z_1, \dots, Z_m depend on the bias. Therefore, received signal vector \mathbf{y} can be expressed as

$$\mathbf{y} = S'_{RT} x + \mathbf{n} \quad (5)$$

where x is the signal emitted by the reader transmitter; it is taken to be a constant scalar. \mathbf{n} is the noise vector. In this experiment, only \mathbf{y} can be observed, not S'_{RT} . The above expressions indicate that altering the load impedances changes the reflected signals. We realize multi-level modulation by setting several different impedance values.

2.2 Experimental System

Figure 3 shows the experimental system model of passive MIMO. In this paper, the transmitted signal is unmodulated continuous wave from a signal generator (SMB 100A SIGNAL GENERATOR). The noise is added in a post-processing step after the experiment, and this noise power is assumed to be sufficiently larger than that observed during the experiment. Figure 4 shows the reader-receiver system. The receiving antennas are connected to the down converter through the low noise amplifier. The down-converter transforms the received RF signals into the baseband I (real) and

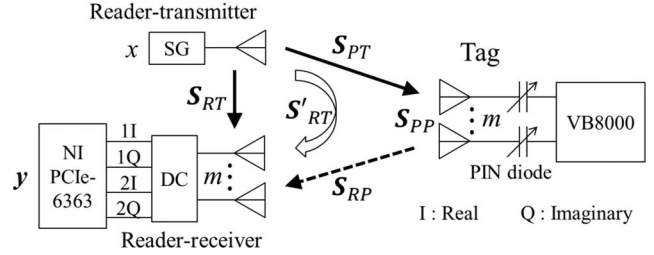


Fig. 3 System model.

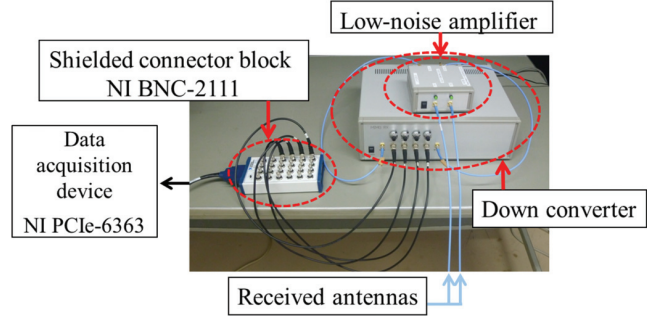


Fig. 4 Reader receiver system.

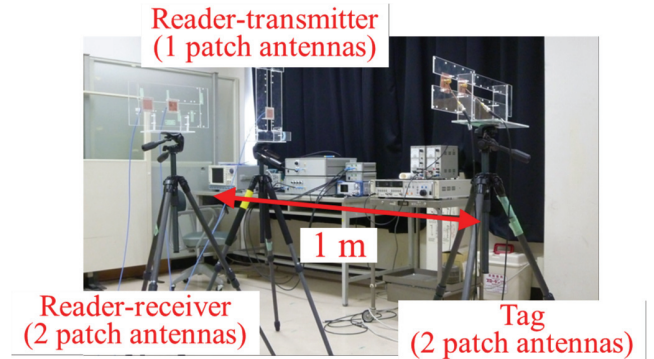


Fig. 5 Experimental setup.

Q (imaginary) part voltages. This system has four baseband ports ($I \times 2 + Q \times 2$) in total since it has two RF receiving ports. The output baseband signals are measured by the data acquisition device (NI PCIe-6363). A computer adds noise to this received signal and calculates the received signal vector, \mathbf{y} . At the tag side, the bias voltages for the PIN diodes are controlled by the waveform generator (YOKOGAWA VB8000 Arbitrary waveform generator). The bias voltages are determined so as that the constellation of reflection coefficients of the PIN diodes are distant from each other.

Figure 5 shows a photo of the experimental setup. In this figure, we conducted the indoor experiment, and used a patch antenna array with $m = 2$. The distance between the reader and the tag is 1 m, and the antenna height was 1.2 m for both the reader and tag. The element spacing was 1λ for both the reader and tag, where λ is wavelength in a vacuum. Figures 6(a), (b) shows close up of the tag an-

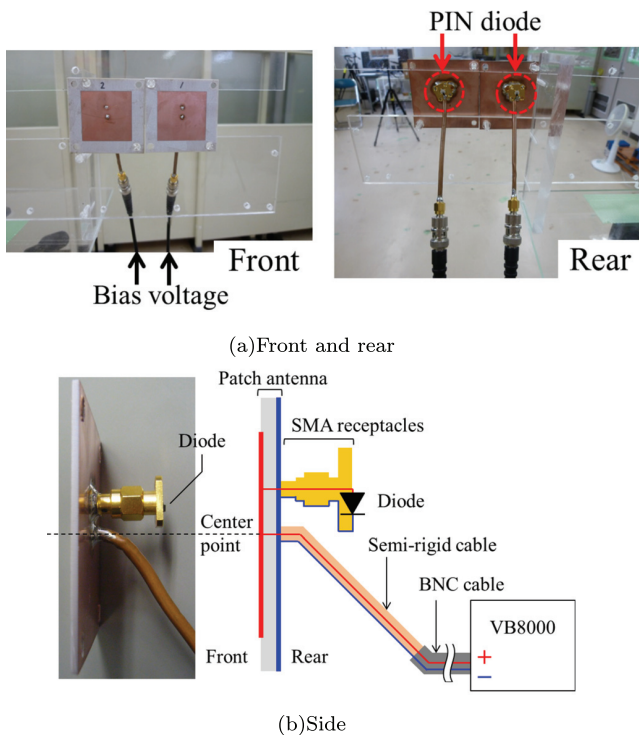


Fig. 6 Tag antenna.

tennas. The PIN diodes are biased by way of the antenna conductor. The bias port is located at the center point of the patch antenna, through which the RF current does not flow. The other side of the PIN diode is connected to the substrate ground through the pin.

Figure 7 shows the sketches of the complex plane that explain the method to determine the reflection coefficients; the continuous line shows the range of reflection coefficients given by the diode. In this case, the number of the bits/symbol is 2, and 4 reflection coefficients are needed. The map of the reflection coefficients can be recognized as the constellation diagram. Note that the locations of the coefficient need to be distant from each other as shown in Fig. 7(a). When the reflection coefficients are determined at random like Fig. 7(b), the distances among the reflection coefficients are closer than that in Fig. 7(a). This yields low noise tolerance since there are only small changes in the reflected signals.

Figure 8 shows the method used to determine the bias voltages; the continuous line shows the coefficient trajectory when the applied voltage to the diode is varied from 0 V to 1.9 V. In Fig. 8(a), '+' represents the determined reflection coefficients, and 4 reflection coefficients (2 bits/symbol/tag-antenna) correspond to 4 bias voltages (0, 0.6, 0.68, 1.9 V). In Fig. 8(b), '+' represents 16 reflection coefficients used when transmission uses 4 bits/symbol/tag-antenna. It can be seen that the distances among the chosen reflection coefficients are much closer than this true for the 2 bits/symbol/tag-antenna case. This suggests that the noise tolerance is lowered if the transmission rate is increased.

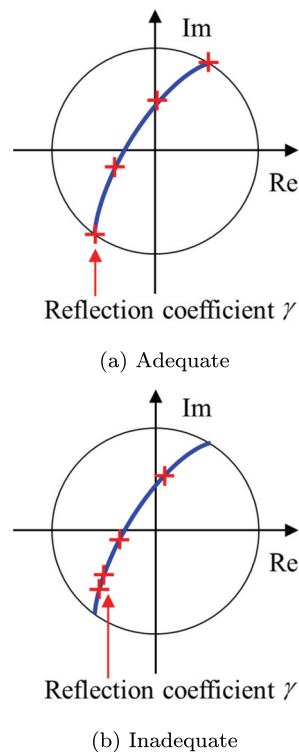


Fig. 7 Determination of reflection coefficients: tag side.

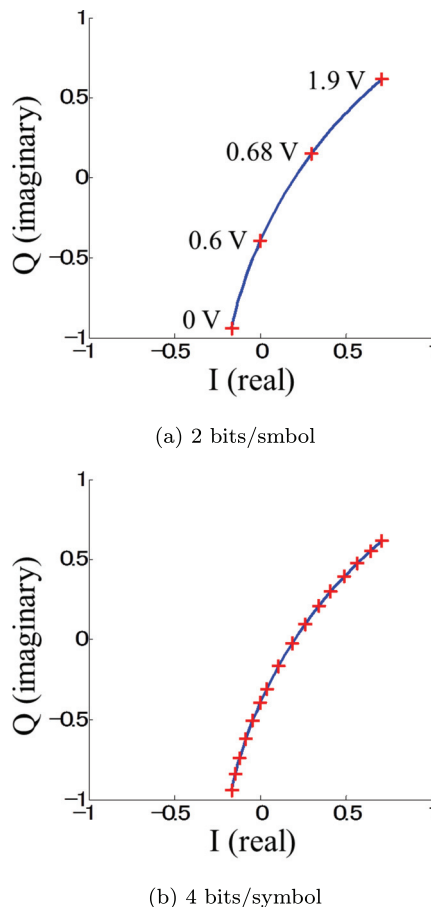


Fig. 8 Determination of diode bias voltages: tag side.

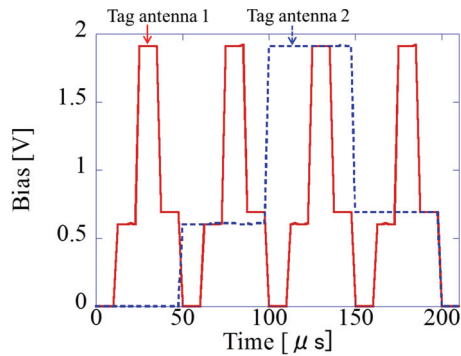


Fig. 9 Time change in bias value.

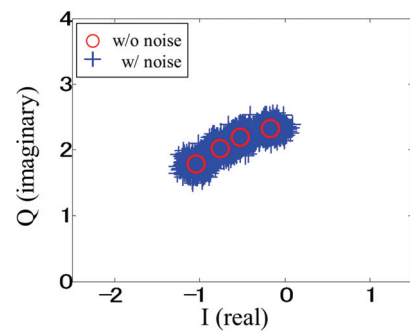
Figure 9 shows temporal transition in bias voltage, where the bias voltage output by the VB8000 is directly measured by the NI PCIe-6363, and the transmission rate is 2 bits/symbol/tag-antenna with $m = 2$. In this figure, the continuous and dashed lines show the biases for tag antennas 1 and 2, respectively. The several different signals are achieved by applying independent voltages to tag antenna 1 and 2. Symbol length is defined as a period wherein the certain termination combination of the biases is given and kept. The symbol rate is 40 kHz. Zero-mean Gaussian white noise was added to the received signal. Maximum likelihood detection (MLD) [12] was used as the decoding algorithm at the reader.

3. Measured Results

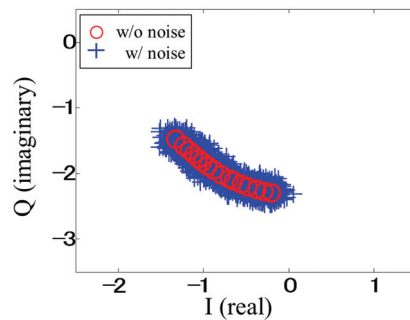
This section discusses the measured results.

We compare the received signals at the reader receiver for SISO (conventional) and 2×2 MIMO. Since the distribution and amplitude range of the received signals vary with changes in antenna position and environment, the distribution of the received signal points shown here is only an example. Figure 10(a) shows the example of the constellation of the received signals when $m = 1$ and the termination impedances are switched among 4 values. The circle is the ideal received signal point obtained by averaging the received signal points in each symbol. The cross is the received signal point that includes noise. This figure indicates that the number of the ideal received signal points is 4; that is, the transmission rate of 2 bits/symbol can be achieved. Figure 10(b) shows the example of the constellation of the received signals when the termination impedances are switched among 16 values. From this figure, the number of ideal received signal points are 16, that is, the transmission rate of 4 bits/symbol can be achieved. The results in Fig. 10(a) show that the signal points are sufficiently separated, so it is easy to demodulate. However, the signal points are close set in Fig. 10(b), which means low noise tolerance.

Next, the results when the number of antennas is increased to $m = 2$ are shown. Figure 11 shows the example of the constellation of the received signals when the termination impedances are switched among 2 values, where

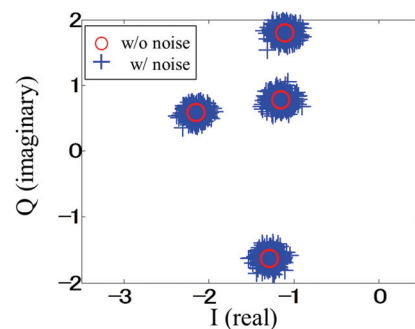


(a) Transmission rate of 2 bits/symbol

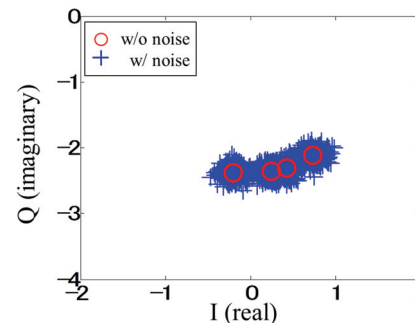


(b) Transmission rate of 4 bits/symbol

Fig. 10 Constellation of received signal in SISO.



(a) Receive antenna 1



(b) Receive antenna 2

Fig. 11 Constellation of received signal in 2×2 MIMO (transmission rate of 2 bits/symbol).

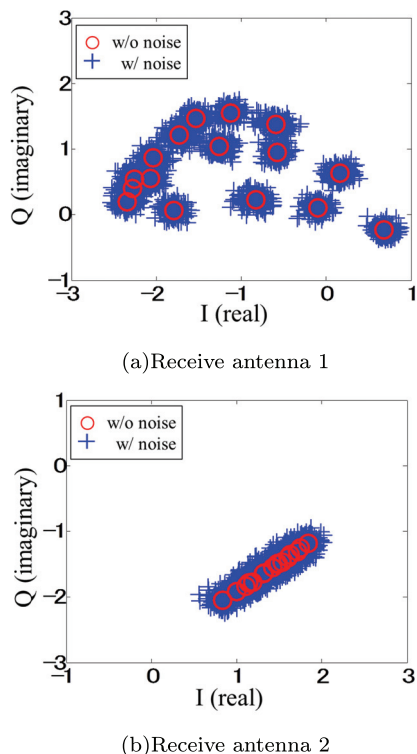


Fig. 12 Constellation of received signal in 2×2 MIMO (transmission rate of 4 bits/symbol).

Figs. 11(a) and (b) show the signals at receiving antenna 1 and 2, respectively. From this figure, the number of ideal received signal points is 4, that is, the transmission rate of 2 bits/symbol can be achieved.

Figure 12 shows the example of the constellation of the received signals when the termination impedances are switched among 4 values. From this figure, the number of ideal received signal points is 16, that is, the transmission rate of 4 bits/symbol can be achieved. Like the result in Fig. 12, the received signal points are likely to overlap each other. Although bit errors may occur if only one received antenna is used in this case, MLD with multiple receiving antennas can distinguish these signals much better than the single antenna receiver.

Figure 13 shows the transmission power versus Bit Error Rate (BER) characteristics for SISO and 2×2 MIMO, where the noise power is -60 dBm. Figure 13(a) shows the result when the distance between the reader and the tag is 0.5 m and 13(b) shows the result when the distance is 1 m. In these figures, the number in parentheses, such as (2 bits \times 1) means (bits per symbol \times the number of tag antenna). Therefore, in both cases of SISO (2 bits \times 1) and 2×2 MIMO (1 bit \times 2), transmission rate is 80 kbits/s. From these results, the transmission power required to achieve the transmission rate of 80 kbits/s with $BER=10^{-2}$ is decreased by 8.4 dB, and that for 160 kbits/s is decreased by 14.9 dB when using MIMO with reader-tag separation distance of 0.5 m. When the distance is 1 m, the transmission power required for 80 kbits/s is decreased by 6.2 dB, and that for 160 kbits/s

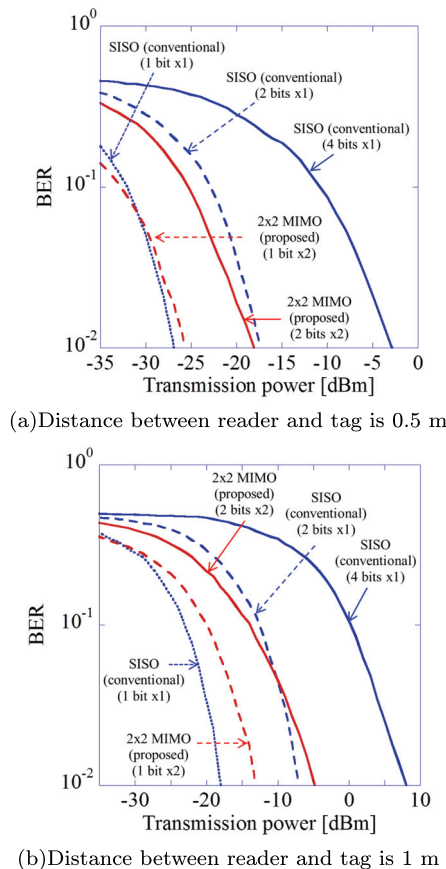


Fig. 13 BER characteristic.

is decreased by 12.3 dB when using MIMO. These results indicate that MIMO has superior BER characteristics compared to SISO regardless of the distance between the reader and the tag, and MIMO is more effective if the required transmission rate is high.

Figure 14 shows the transmission power with $BER=10^{-2}$ versus the transmission rate for SISO and 2×2 MIMO, where the noise power is -60 dBm. Figures 14(a) and (b) show the results when the distances between the reader and the tag are 0.5 m and 1 m, respectively. These results indicate that MIMO is more effective if the required transmission rate is high, and that the transmission rate of passive MIMO is up to 2 times higher than that of SISO for the same transmission power when the distance between the reader and the tag is 0.5 m. When the distance is 1 m, the transmission rate of MIMO is up to 1.7 times higher than that of SISO. These results indicate that passive MIMO offers high-speed data transmission.

Figure 15 shows the BER characteristics when the distance between the reader and the tag is varied; the transmission power is 10 dBm, the noise power is -60 dBm, and the transmission rate is 160 kbits/s. The results show that the available distances in MIMO and SISO are 1.7 m and 1.1 m, respectively. This means that passive MIMO can improve the transmission distance because it realizes spatial diversity gain through the use of multiple antennas.

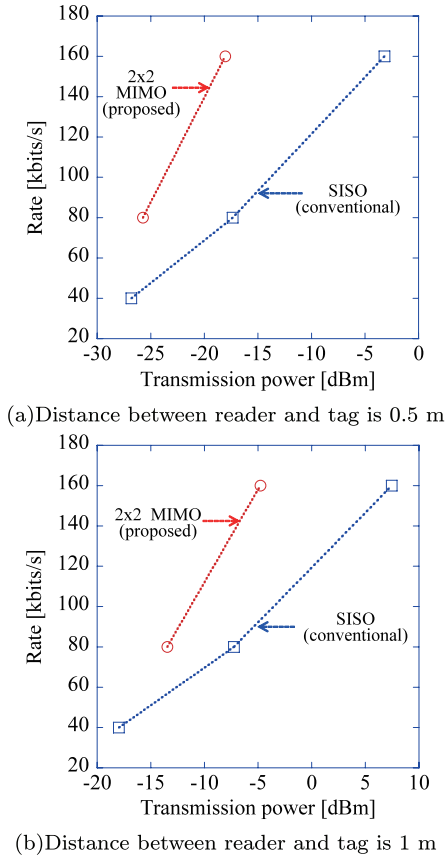


Fig. 14 Transmission power versus transmission rate.

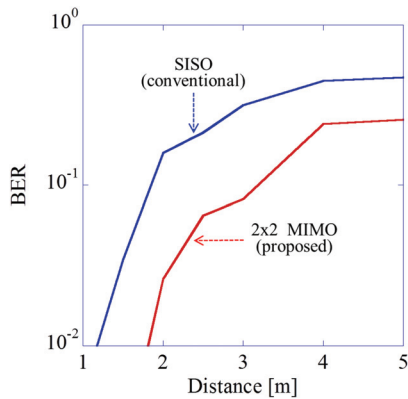


Fig. 15 Distance characteristic.

4. Conclusion

In this paper, we presented the results of experiments on our passive MIMO transmission proposal, which uses load modulation and MIMO techniques, and proved its validity. PIN diodes are used as the variable impedance elements at the tag side to achieve multi-level modulation. The measured transmission rate of passive MIMO is up to 2 times that of SISO at the same transmission power when the distance between the reader and the tag is 0.5 m. When the distance

is 1 m, MIMO is up to 70% faster than SISO. These results indicate that passive MIMO is superior to the conventional load modulation scheme for realizing high-speed and long-distance RFID systems.

Acknowledgements

This research was partially supported by JSPS KAKENHI (25709030).

References

- [1] V. Chawla and D.S. Ha, "An overview of passive RFID," *IEEE Commun. Mag.*, vol.45, no.9, pp.11–17, Sept. 2007.
- [2] M.A. Ingram, M.F. Demirkol, and D. Kim, "Transmit diversity and spatial multiplexing for RF links using modulated backscatter," *Proc. International Symposium on Signals, Systems, and Electronics* 2001.
- [3] J.D. Griffin and G.D. Durgin, "Gains for RF tags using multiple antennas," *IEEE Trans. Antennas Propag.*, vol.56, no.2, pp.563–570, Feb. 2008.
- [4] I.E. Teletar, "Capacity of multi-antenna Gaussian channels," *Tech. Rep. AT*, T-Bell Labs, June 1995.
- [5] G.J. Foschini, "Layered space-time architecture for wireless communication in a fading environment when using multielement antennas," *Bell Labs Tech. J.*, pp.41–59, Autumn 1996.
- [6] S.K. Jayaweera and H.V. Poor, "On the capacity of multiple-antenna systems in Rician fading," *IEEE Trans. Wireless Commun.*, vol.4, no.3, pp.1102–1111, May 2005.
- [7] Y. Karasawa, "Innovative antennas and propagation studies for MIMO systems," *IEICE Trans. Commun.*, vol.E90-B, no.9, pp.2194–2202, Sept. 2007.
- [8] A. Goldsmith, S.A. Jafar, N. Jindal, and S. Vishwanath, "Capacity limits of MIMO channels," *IEEE J. Sel. Areas Commun.*, vol.21, no.5, pp.684–702, June 2003.
- [9] K. Terasaki and N. Honma, "Feasible load modulation technique using multiple antenna systems," *IET Journals Electronics Letters*, vol.48, no.18, pp.1090–1091, Aug. 2012.
- [10] K. Terasaki, K. Kinami, and N. Honma, "Passive MIMO transmission using load modulation," *2012 International Symposium on Antennas and Propagation (ISAP 2012)*, Electric Proc. ISAP 2012, POS2-27, Oct. 2012.
- [11] K. Terasaki and N. Honma, "Experimental study on passive MIMO transmission," *2012 Asia-Pacific Microwave Conference (APMC 2012)*, Electric Proc. APMC 2012, 4B3-08 1031-1033, Dec. 2012.
- [12] A. van Zelst, R. van Nee, and G.A. Awater, "Space division multiplexing (SDM) for OFDM systems," *Vehicular Technology Conference Proceedings*, 2000. VTC 2000-Spring Tokyo. 2000 IEEE 51st, vol.2, pp.1090–3038, May 2000.



Keisuke Terasaki received the B.E. degree in electrical and electronic engineering from Iwate University, Morioka, Japan in 2012. He is currently in the master program in Iwate University. His research interest is feasible load modulation techniques for multiple antenna systems.



Naoki Honma received the B.E., M.E., and Ph.D. degrees in electrical engineering from Tohoku University, Sendai, Japan in 1996, 1998, and 2005, respectively. In 1998, he joined the NTT Radio Communication Systems Laboratories, Nippon Telegraph and Telephone Corporation (NTT), in Japan. He is now working for Iwate University. He received the Young Engineers Award from the IEICE of Japan in 2003, the APMC Best Paper Award in 2003, and the Best Paper Award of IEICE Communication Society in 2006, respectively. His current research interest is planar antennas for high-speed wireless communication systems. He is a member of IEEE.